Initial burst of oceanic crust accretion in the Red Sea due to edge-driven mantle convection

Marco Ligi[1]*, Enrico Bonatti[1,2], Fabio Caratori Tontini[3], Anna Cipriani[2,4], Luca Cocchi[5], Antonio Schettino[6], Giovanni Bortoluzzi[1], Valentina Ferrante[1], Samir Khalil[7], Neil C. Mitchell[8], and Najeeb Rasul[9]

[1]Istituto di Scienze Marine, Consiglio Nazionale delle Ricerche, Via Gobetti 101, 40129 Bologna, Italy
[2]Lamont Doherty Earth Observatory, Columbia University, Palisades, New York 10964, USA
[3]GNS Science, Ocean Exploration Section, 1 Fairway Drive, Avalon, Lower Hutt 5040, New Zealand
[4]Dipartimento di Scienze della Terra, Università di Modena, Largo S. Eufemia 19, 41100 Modena, Italy
[5]Istituto Nazionale di Geofisica e Vulcanologia, Roma2, Via Pezzino Basso 2, 19020 Fezzano (La Spezia), Italy
[6]Dipartimento di Scienze della Terra, Università di Camerino, Via Gentile III da Varano, 62032 Camerino, Italy
[7]Department of Geological and Biological Sciences, Suez Canal University, El Arish Branch, Egypt
[8]School of Earth, Atmospheric and Environmental Sciences, University of Manchester, Williamson Building, Oxford Road, Manchester M13 9PL, UK
[9]Saudi Geological Survey, 21514 Jeddah, Saudi Arabia

ABSTRACT

The 500 m.y. cycle whereby continents assemble in a single supercontinent and then fragment and disperse again involves the rupturing of a continent and the birth of a new ocean, with the formation of passive plate margins. This process is well displayed today in the Red Sea, where Arabia is separating from Africa. We carried out geophysical surveys and bottom rock sampling in the two Red Sea northernmost axial segments of initial oceanic crust accretion, Thetis and Nereus. Areal variations of crustal thickness, magnetic intensity, and degree of melting of the subaxial upwelling mantle reveal an initial burst of active oceanic crust generation and rapid seafloor spreading below each cell, occurring as soon as the lid of continental lithosphere breaks. This initial pulse may be caused by edge-driven subrift mantle convection, triggered by a strong horizontal thermal gradient between the cold continental lithosphere and the hot ascending asthenosphere. The thermal gradient weakens as the oceanic rift widens; therefore the initial active pulse fades into steady, more passive crustal accretion, with slower spreading and along axis rift propagation.

INTRODUCTION

The Wilson Cycle of continent assemblage and dispersal (Wilson, 1966) includes rifting of continental blocks that can lead to the birth of new oceans. Interaction of structural and magmatic processes during continental rifting and breakup results in a variety of rift systems ranging from narrow to wide, and from magma dominated to magma starved (Hopper and Buck, 1998; Eldholm and Grue, 1994; Whitmarsh et al., 2001). Mechanisms of crustal accretion at mid-ocean ridges are fairly well established, and suggest a general dependence of crustal production on spreading rate. However, relationships between rifting and magmatism, the initial generation of oceanic crust and the transition from rifting to spreading, are still poorly constrained (Lizarralde et al., 2007; Armitage et al., 2009). We addressed these issues in the Red Sea Rift, where the rupturing of a continent and the birth of a new ocean are occurring today with the separation of Arabia from Africa. Since Late Oligocene–Miocene time, a rift system has been fragmenting the Arabian-Nubian shield, which consists of ancient island arc and backarc basins, continental microplates, and interlaying ocean basins, welded together during the Proterozoic Pan-African orogenic cycle (Ghebreab, 1998). The impingement of the Afar mantle plume from below, starting ca. 40 Ma, may have influenced the evolution of the system (Ebinger and Sleep, 1998), although there has been little volcanism within the central-northern Red Sea Rift since the Early Miocene. A nearly continuous axial valley carpeted by basaltic oceanic crust and flanked by Vine-Matthews magnetic anomalies as old as 5 Ma extends for ~400 km in the southern Red Sea (Roeser, 1975). It becomes discontinuous in the central Red Sea where the initial emplacement of oceanic crust occurs in discrete axial cells (Bonatti, 1985), and is absent in the northern Red Sea (Fig. 1), although scattered basaltic intrusions have been observed there (Cochran, 2005).

FIELD WORK

With the R/V *Urania*, we carried out multibeam, magnetic, and multichannel seismic reflection surveys as well as bottom rock sampling, focusing on the two northernmost Red Sea axial oceanic cells, i.e., Thetis and Nereus Deeps (Fig. 1). These two rift valley segments, emplaced within the sedimentary-evaporitic sequence ubiquitous in the Red Sea, are separated by a non-oceanic inter-trough zone. Gravity, bathymetry, and sediment thickness data were used to calculate the mantle Bouguer anomaly (MBA) (see the GSA Data Repository[1]). Inversion of the MBA after removal of the predicted thermal gravity field, as well as magnetic anomalies, gave us the areal distribution of crustal thickness and intensity of rock magnetization, together with crustal ages and spreading rates (Fig. 2).

Thetis Deep

We found that Thetis Deep, a 65-km-long, ~2200-m-deep axial valley, is actually made by the coalescence of three slightly offset subbasins that become shallower and narrower from south to north (Fig. 1). The >1-km-high valley walls show step-like morphology, probably an expression of extensional normal faults partly smoothed by down-slope sliding of Miocene evaporites (Mitchell et al., 2010).

The Thetis southern subbasin is floored by a strongly magnetic axial neovolcanic ridge and by numerous small central volcanoes. Two negative symmetric magnetic anomalies flank the axial anomaly (anomaly c1n) in the southernmost part of Thetis southern subbasin, suggesting an initial emplacement of oceanic crust as early as 2.2 Ma, with an average full spreading rate of ~16 mm yr^{-1}, ranging from 23 mm yr^{-1} during the Matuyama chron to 8 mm yr^{-1} during the Brunhes chron. Intervals of higher spreading rates correspond to areas of thicker crust (Fig. 2). Moving north within the southern subbasin, the negative anomalies flanking the axial anomaly disappear, implying a more recent onset of oceanic crustal accretion.

*E-mail: marco.ligi@bo.ismar.cnr.it.

[1]GSA Data Repository item 2011302, supplemental methods, is available online at www.geosociety.org/pubs/ft2011.htm, or on request from editing@geosociety.org or Documents Secretary, GSA, P.O. Box 9140, Boulder, CO 80301, USA.

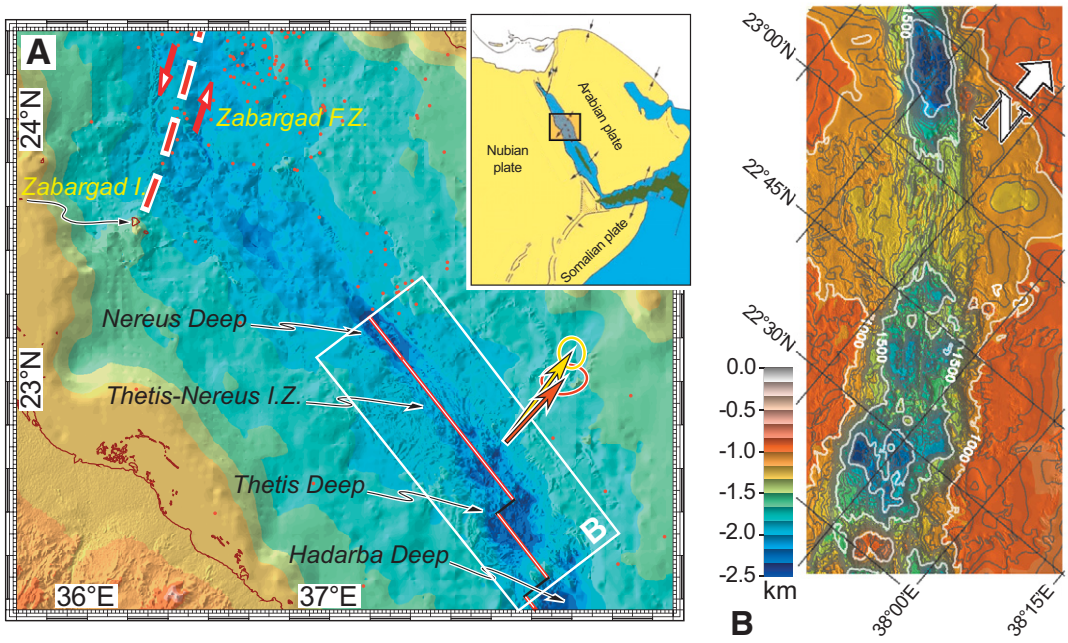

Figure 1. A: Topography of northern-central Red Sea. Red dots—earthquake epicenters from International Seismological Data Centre. Red lines—axes of Nereus and Thetis segments. Yellow and orange arrows indicate velocity vectors of Arabia relative to Nubia plate from Chu and Gordon (1998), and from ArRajehi et al. (2010), with full spreading rate of 12.1 mm yr^{-1} (an average for past 3 m.y.) and 10.5 mm yr^{-1} (global positioning system–based present-day rate), respectively. F.Z.—fracture zone. Top right inset: simplified plate tectonic framework of Red Sea–Gulf of Aden area; dark areas are oceanic crust. B: Shaded relief image showing that Thetis segment consists of three right-stepped subbasins. Axial depression broadens significantly in Thetis-Nereus intertrough zone relative to oceanic segments: 1000 m isobath encloses axial area ~80 km wide at intertrough zone, but only 40 and 30 km wide at Nereus and Thetis, respectively. This pattern indicates that deformation becomes focused in a narrow axial zone at initiation of oceanic accretion.

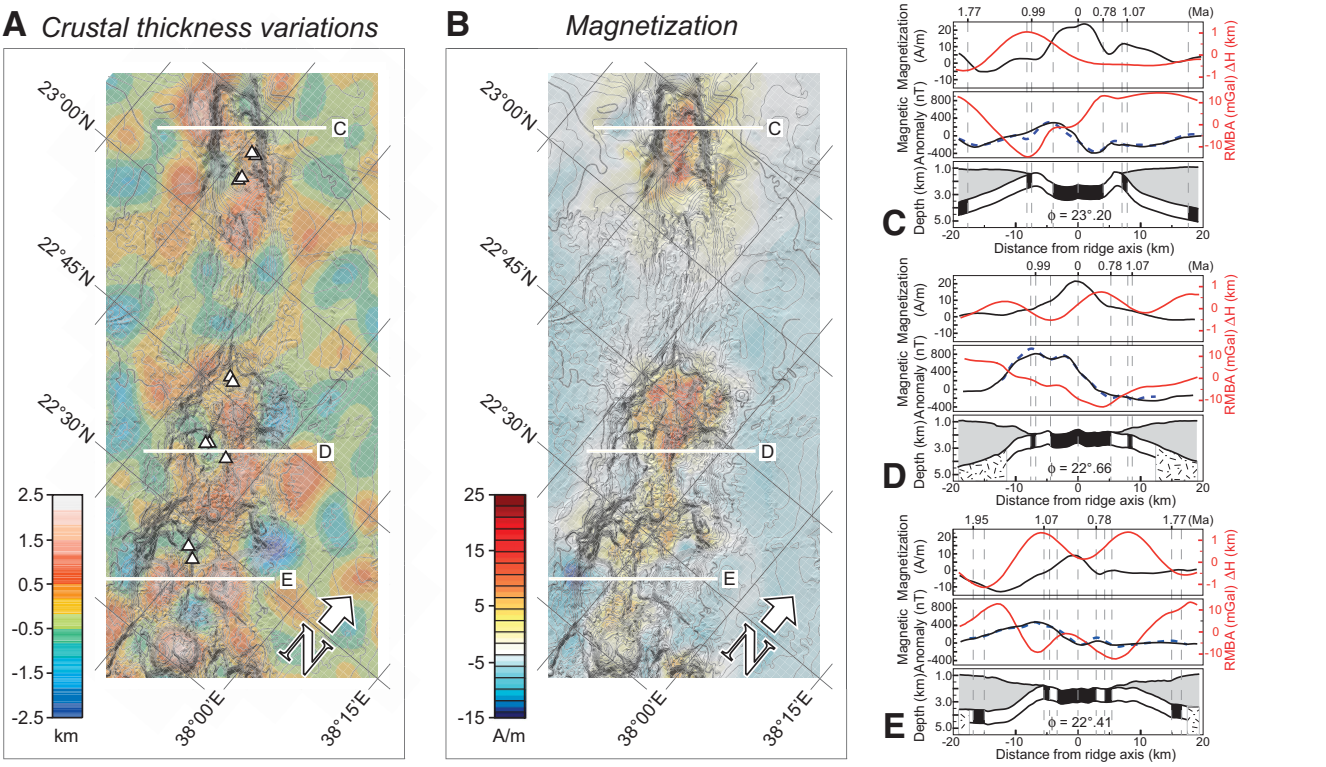

Figure 2. Inversion of gravity and magnetic data superimposed on bathymetry and across-axis geophysical profiles from Thetis and Nereus. A: Crustal thickness variations obtained after downward continuation of a low-pass filtered set (wavelengths <12 km were filtered out) of computed residual mantle Bouguer anomalies (RMBAs) to depth of 8 km below sea level. MBA was generated by subtracting from computed free-air anomalies the attraction of seafloor topography, sediments, and evaporites, and the crust-mantle interface, assuming 5-km-thick crust and densities of 1040, 1900, 2200, 2690, and 3330 kg m^{-3} for seawater, sediments, evaporites, crust, and mantle, respectively. White triangles—locations of rock samples shown in Figure 3. B: Intensity of rock magnetization obtained by inversion of reduced-to-pole magnetic anomalies assuming 1-km-thick magnetic layer parallel to bottom of evaporite layer. C, D, E: Gravity and magnetic profiles across midsegment points of Nereus and Thetis central and southern subbasins, respectively; profile locations are indicated by labeled lines in A and B. Latitude of each profile at ridge axis = ϕ. Bottom—geological model. Gray shaded area—sediment and evaporite layer. Black and white stripes—normal and reverse geomagnetic events. Hachure pattern—transitional crust. Geomagnetic scale is from Cande and Kent (1995). Center—observed (black line) and synthetic (blue dashed line) magnetic anomalies, and RMBA (red line). Top—inferred variations of rock magnetization (black line) and crustal thickness (red line).

The central subbasin, in addition to having scattered small volcanoes, has a strongly magnetic axial neovolcanic zone, flanked only by narrow symmetrical negative anomalies; this suggests initial emplacement of oceanic crust ca. 1.6 Ma, with an average spreading rate of 15 mm yr^{-1}, affected by a slight asymmetry (~10% faster to the east). Crustal thickness shows a positive linear anomaly slightly east of the ridge axis (Fig. 2).

The northern subbasin does not show a clearly defined linear neovolcanic zone, although it displays a strong central magnetization, suggesting a recent (younger than 0.78 Ma) initial breakthrough of oceanic crust.

Nereus Deep

Nereus Deep is an ~50-km-long, ~2500-m-deep axial rift valley (Fig. 1) flanked by >1 km walls with step-like morphology due to normal faults partly masked by salt tectonics at segment ends. The ~12-km-wide valley floor is dissected by an ~250-m-high neovolcanic axial ridge that exposes fresh oceanic-type basalts, with a strong central magnetic anomaly. At mid-segment point, the central anomaly is flanked by symmetrical reversed anomalies (Matuyama chron) that vanish toward segment ends. Crustal thickness is at a maximum in the areas of reversed magnetization; toward the southeast, the maximum thickness shifts toward the axis of the basin (Fig. 2). Thus, the Nereus oceanic cell started ca. 2 Ma, roughly the same time as the initial activation of the southern Thetis cell. The average full spreading rate is 20 mm yr^{-1}; the maximum was 26 mm yr^{-1} during the Matuyama chron, and slowed to 10 mm yr^{-1} during the Brunhes chron.

Thetis-Nereus Intertrough Zone

This ~35-km-long intertrough zone is marked by a broad, gentle axial depression, carpeted by sediments and devoid of volcanism and linear magnetic anomalies. It displays curvilinear ridge-trough topography aligned in a Red Sea direction (Fig. 1), probably due to folding of the sedimentary sequence, caused by evaporite flow toward the rift axis (Mitchell et al., 2010). We infer that the Thetis-Nereus intertrough zone consists of stretched and thinned continental crust, probably injected by diffuse basaltic intrusions, capped by Miocene evaporitic and Pliocene–Quaternary biogenic sediments.

INITIAL BURST OF OCEANIC ACCRETION

The initial breakthrough of new oceanic crust is occurring today (i.e., after 0.7 Ma) in the Thetis northern subbasin and in the southern tip of Nereus, with an intensity of magnetization almost twice that of the near-zero-age axial zones of the Thetis central and southern subbasins, where the initial emplacement of oceanic crust occurred 1.6 and 2.2 Ma, respectively. This higher magnetization is not due to crustal composition, because it is associated with basalts that are not enriched in Fe relative to basalts from the central and southern subbasins (Fig. 3B); therefore, it must be due to a thicker basaltic crust, as suggested independently by the areal distribution of crustal thickness inferred from gravity (Fig. 2).

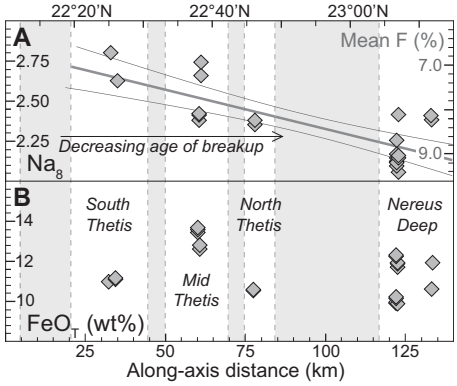

Figure 3. Along-axis variations of degree of melting (from basalt Na_8) and basalt Fe content. Profile location is in Figure 1 (red line). A: Na_8 of basaltic glasses and mantle degree of melting estimated from Na_8 assuming pure-fractional melting regime and complete melt extraction (Ligi et al., 2005). Na_2O normalized to 8 wt% MgO, according to Plank and Langmuir (1992). B: Total FeO of basaltic glasses.

Basaltic glasses from areas of thicker crust, i.e., Thetis northern subbasin and southern tip of Nereus, have an Na_8 content lower than glasses from the axis of the Thetis central and southern subbasins (Fig. 3A). Basalt Na_8 is inversely related to the mantle degree of melting by which the basalt was generated (Klein and Langmuir, 1987). Thus, these initial oceanic basalts were generated by a mantle degree of melting higher than that of the basalts produced today in the more evolved Thetis central and southern subbasins. The degree of melting of Nereus basalts decreases toward the axial mid-segment point, where oceanization started ca. 2.0 Ma. Degree of melting versus age of the initial breakthrough of oceanic crust shows that initial basalts were generated by a degree of melting higher than that of subsequent melts (Fig. 3A). Moreover, spreading velocities in the Thetis southern basin and Nereus were highest immediately after the initial breakthrough of oceanic crust, and then slowed.

These results indicate an intense initial pulse of oceanic crust generation and fast spreading as soon as the lid of thinned continental lithosphere cracks up (Fig. 4). An initial pulse could be caused either by higher temperature and/or fertility of the ascending subrift asthenosphere (Lizarralde et al., 2007; Armitage et al., 2009), or by its increased, active ascending velocity triggered by secondary convection. If the initial mantle degree of melting were due to a passive upwelling regime, similar to that prevalent along mid-ocean ridges, given a 6.1 mm/yr Red Sea half-spreading rate (Chu and Gordon, 1998), mantle temperatures 60–80 °C higher than the ~1350 °C value assumed for the source of mid-oceanic ridge basalt (MORB) would be required, with 3–4 times faster spreading. These higher temperatures would deepen the peridotite solidus and the initiation of melting, thus increasing the average pressure of melting. Basalt Fe_8, thought to reflect the average pressure of melting, suggests that, for MORB, high degrees of melting go together with high average melting pressure (Klein and Langmuir, 1987). In contrast, basalt Fe_8 correlates positively with Na_8 both at Thetis and Nereus (Fig. 4D); i.e., high degrees of melting go together with low average pressures of melting. This suggests that high mantle temperature and/or fertility is not the main cause of the Red Sea Rift initial melting pulse.

Our explanation is that initial mantle upwelling below Thetis and Nereus is enhanced by secondary small-scale mantle convection, triggered by a sharp horizontal thermal gradient between the thick and cold continental lithospheric walls and the hot asthenosphere rising below rift axis (Fig. 4B). The narrow central Red Sea transition zone from thick continental lithosphere to initial oceanic lithosphere (~50 km) contrasts with margins with wide continental to oceanic zones of transition (Hopper and Buck, 1998; Whitmarsh et al., 2001). An example is the >200-km-wide Iberian margin, with scarce or absent initial oceanic basalt injections, slow initial spreading, and mostly passive mantle upwelling (Srivastava et al., 2000). Both wide and nonmagmatic, and narrow and magmatic, rift segments are observed in the Gulf of California (Lizarralde et al., 2007) and Gulf of Aden (D'Acremont et al., 2006) rifts.

Secondary mantle convection, predicted below narrow rifts (Buck, 1986; Boutilier and Keen, 1999), should weaken as the oceanic rift widens, decreasing the horizontal thermal gradient. This would explain why the initial melting and/or spreading pulse declines rapidly at each Red Sea cell, being replaced by a more passive steady regime of mantle upwelling and crustal accretion (Fig. 4C). This model explains the relatively thick oceanic crust and fast spreading at both edges of the Thetis southern subbasin, associated with the oldest magnetic anomalies (Fig. 2E). Initial spreading in the eastern Gulf of Aden rift at magnetic anomaly c5Dn (ca. 17 Ma) appears to have been faster than subsequent spreading (D'Acremont et al. 2006), in accordance with our Red Sea model.

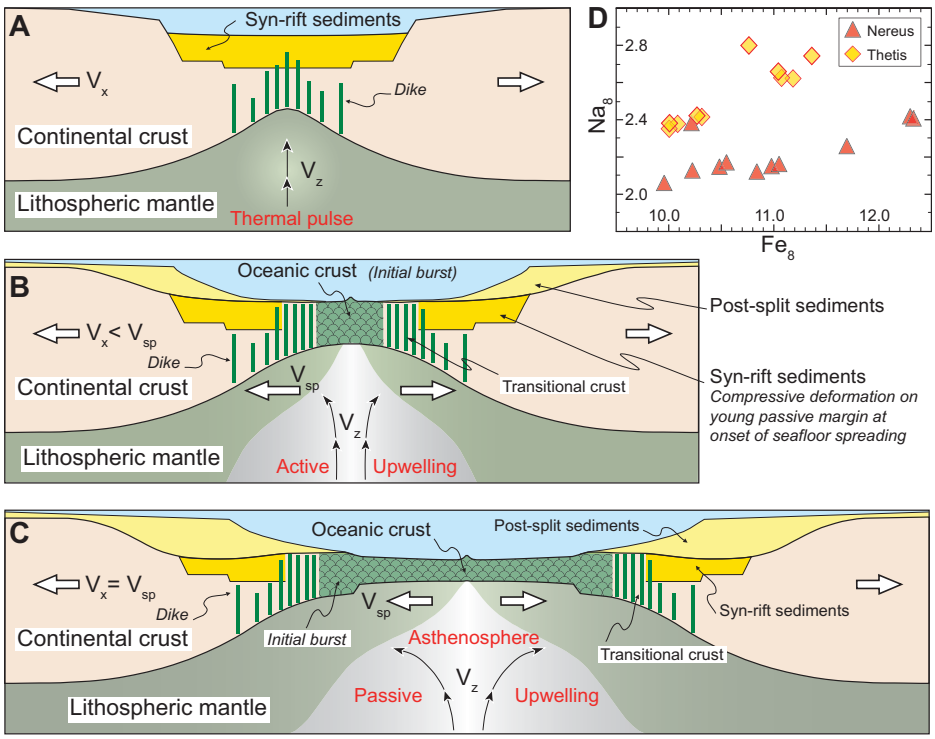

Figure 4. Continental to oceanic rift transition in central Red Sea. A: During continental rifting, thermal and/or compositional anomaly, probably related to Afar plume (Ebinger and Sleep, 1998), developed beneath lithosphere. B: Increased temperatures deepen solidus and favor short-lived small-scale convection by locally decreasing viscosity and increasing buoyancy of upwelling asthenosphere. Strong horizontal thermal gradient enhances secondary mantle convection, causing initial burst of oceanic crust injection, with high degree of melting, thick crust, and fast spreading. C: Excess thermal anomaly decays rapidly as oceanic rift widens and horizontal thermal gradient decreases, evolving into more passive steady regime dictated by spreading rate. V_{sp} is the oceanic crustal accretion rate; V_z and V_x are mantle upwelling and plate separation velocities, respectively. D: Distribution of Na_8 and Fe_8 in mid-oceanic ridge basalt glasses along axes of Thetis and Nereus. FeO compositions at common 8 wt% MgO were calculated using equation of Klein and Langmuir (1987).

A burst of active mantle upwelling at the onset of oceanic crust injection, followed by passive drifting, may be common during the breakup of continents: for example, it may have occurred in narrow Red Sea–type segments of continent-ocean transition during the Mesozoic separation of North America and Europe-Africa (Armitage et al. 2009; Withjack et al., 1998), in contrast with wide, Iberian-type rift segments.

ACKNOWLEDGMENTS

This research was sponsored by the Eurocore-Euromargins Programme (Project 01-LEC-EMA21F) and Programma Giovani Ricercatori Rita Levi Montalcini. We thank Captain E. Gentile and the officers and crew of the R/V *Urania* for their collaboration during the field work. This work was supported by the Italian Consiglio Nazionale Ricerche and the U.S. National Science Foundation.

REFERENCES CITED

Armitage, J.J., Henstock, T.J., Minshull, T.A., and Hopper, J.R., 2009, Lithospheric controls on melt production during continental breakup at slow rates of extension: Application to the North Atlantic: Geochemistry Geophysics Geosystems, v. 10, Q06018, doi:10.1029/2009GC002404.

ArRajehi, A., and 16 others, 2010, Geodetic constraints on present day motion of the Arabian Plate: Implications for Red Sea and Gulf of Aden rifting: Tectonics, v. 29, TC3011, doi:10.1029/2009TC002482.

Bonatti, E., 1985, Punctiform initiation of seafloor spreading in the Red Sea during transition from continental to an oceanic rift: Nature, v. 316, p. 33–37, doi:10.1038/316033a0.

Boutilier, R.R., and Keen, C.E., 1999, Small scale convection and divergent plate boundaries: Journal of Geophysical Research, v. 104, p. 7389–7403, doi:10.1029/1998JB900076.

Buck, W.R., 1986, Small-scale convection induced by passive rifting: The cause for uplift of rift shoulders: Earth and Planetary Science Letters, v. 77, p. 362–372, doi:10.1016/0012-821X(86)90146-9.

Cande, S.C., and Kent, D.V., 1995, Revised calibration of the geomagnetic polarity time scale for the Late Cretaceous and Cenozoic: Journal of Geophysical Research, v. 100, p. 6093–6095, doi:10.1029/94JB03098.

Chu, D., and Gordon, R.G., 1998, Current plate motions across the Red Sea: Geophysical Journal International, v. 135, p. 313–328, doi:10.1046/j.1365-246X.1998.00658.x.

Cochran, J.R., 2005, Northern Red Sea: Nucleation of an oceanic spreading center within a continental rift: Geochemistry Geophysics Geosystems, v. 6, Q03006, doi:10.1029/2004GC000826.

D'Acremont, E., Leroy, S., Maia, M., Patriat, P., Berslier, M.O., Bellahsen, N., Fournier, M., and Gente, P., 2006, Structure and evolution of the eastern Gulf of Aden: Insights from magnetic and gravity data: Geophysical Journal International, v. 165, p. 786–803, doi:10.1111/j.1365-246X.2006.02950.x.

Ebinger, C.J., and Sleep, N.H., 1998, Cenozoic magmatism throughout east Africa resulting from impact of a single plume: Nature, v. 395, p. 788–791, doi:10.1038/27417.

Eldholm, O., and Grue, K., 1994, North Atlantic volcanic margins: Dimensions and production rates: Journal of Geophysical Research, v. 99, p. 2955–2968, doi:10.1029/93JB02879.

Ghebreab, W., 1998, Tectonics of the Red Sea region reassessed: Earth-Science Reviews, v. 45, p. 1–44, doi:10.1016/S0012-8252(98)00036-1.

Hopper, J.R., and Buck, W.R., 1998, Styles of extensional decoupling: Geology, v. 26, p. 699–702, doi:10.1130/0091-7613(1998)026<0699:SOED>2.3.CO;2.

Klein, E.M., and Langmuir, C.H., 1987, Global correlations of ocean ridge basalt chemistry with axial depth and crustal thickness: Journal of Geophysical Research, v. 92, p. 8089–8115, doi:10.1029/JB092iB08p08089.

Ligi, M., Bonatti, E., Cipriani, A., and Ottolini, L., 2005, Water-rich basalts at mid-ocean-ridge cold spots: Nature, v. 434, p. 66–69, doi:10.1038/nature03264.

Lizarralde, D., Axen, G.J., Brown, H.E., Fletcher, J.M., González-Fernández, A., Harding, A.J., Holbrook, W.S., Kent, G.M., Paramo, P., Sutherland, F., and Umhoefer, P.J., 2007, Variation in styles of rifting in the Gulf of California: Nature, v. 448, p. 466–469, doi:10.1038/nature06035.

Mitchell, N.C., Ligi, M., Bonatti, E., Brunelli, D., Ferrante, V., and Rutter, E., 2010, Submarine salt flows in the central Red Sea: Geological Society of America Bulletin, v. 122, p. 701–713, doi:10.1130/B26518.1.

Plank, T., and Langmuir, C.H., 1992, Effects of the melting regime on the composition of oceanic crust: Journal of Geophysical Research, v. 97, p. 19749–19770, doi:10.1029/92JB01769.

Roeser, H.A., 1975, A detailed magnetic survey of the southern Red Sea: Geologisches Jahrbuch, v. 13, p. 131–153.

Srivastava, S.P., Sibuet, J.-C., Cande, S., Roest, W.R., and Reid, I.D., 2000, Magnetic evidence for slow seafloor spreading during the formation of the Newfoundland and Iberian margins: Earth and Planetary Science Letters, v. 182, p. 61–76, doi:10.1016/S0012-821X(00)00231-4.

Whitmarsh, R.B., Manatschal, G., and Minshull, T.A., 2001, Evolution of magma-poor continental margins from rifting to seafloor spreading: Nature, v. 413, p. 150–154, doi:10.1038/35093085.

Wilson, J.T., 1966, Did the Atlantic close and then re-open?: Nature, v. 211, p. 676–681, doi:10.1038/211676a0.

Withjack, M.O., Schlische, R.W., and Olsen, P.E., 1998, Diachronous rifting, drifting and inversion on the passive margin of central eastern North America: An analog for other passive margins: American Association of Petroleum Geologists Bulletin, v. 82, p. 817–835.

Manuscript received 10 March 2011
Revised manuscript received 27 May 2011
Manuscript accepted 14 June 2011

Printed in USA